Optical properties of excitons under an axial-potential perturbation

Q. X. Zhao and T. Westgaard
Department of Physics, University of Trondheim–NTH, N-7034 Trondheim, Norway
(Received 16 January 1991)

The optical properties and electronic structure of isoelectronic defect bound excitons in semiconductors have been studied. A simple model is used to describe the electron-attractive and hole-attractive isoelectronic defects. This effective-perturbation Hamiltonian model gives a clear physical picture of the two extreme cases of hole-attractive isoelectronic defect bound excitons, i.e., where the total angular momentum of the bound hole is unchanged ($J=\frac{3}{2}$) and where the orbital angular momentum of the bound hole has been quenched ($J=\frac{1}{2}$). This model can also be applied to quantum-well (QW) structures. Optical properties of the lowest heavy–light-hole state related excitons in QW's such as transition probabilities, splitting of exciton states in a magnetic field, and exchange splitting are also discussed within this model. By analyzing the experimental data with magnetic fields up to 18 T for 90-Å $GaAs/Al_{0.26}Ga_{0.74}As$ QW's, the g values of electrons and holes are estimated to $g_e=-0.26\pm0.05$ for electrons and $g_h=0.58\pm0.05$ for holes.

I. INTRODUCTION

Studies of electronic structure and optical properties of isoelectronic defects in semiconductors are interesting both from an experimental and a theoretical point of view. Many such isoelectronic defects have been studied during the past two decades, e.g., isoelectronic defects in GaP,[1–5] ZnTe,[6–9] Si,[10] and GaAs.[11] No first-principles theory exists yet, but many properties of such defects are understood from several experiments and simple models.[12] The most widely accepted model is the Hopfield-Thomas-Lynch (HTL) model,[13] in which the first charged particle is attracted by a short-range impurity and/or defect potential, and then the second charged particle is attracted by the Coulomb potential of the first particle. Thus the defects can be classified as electron- or hole-attractive isoelectronic defects according to whether the first bound particle is an electron or a hole. For the hole-attractive isoelectronic defects, two extreme cases have been found in experiments. In the first case the bound hole has an angular momentum $J=\frac{3}{2}$, and in the other case the bound hold has an angular momentum $J=\frac{1}{2}$ and is characterized as spinlike. In the latter case the hole's orbital angular momentum is said to be quenched by the crystal potential.

In this paper the transition between the two extreme cases for hole-attractive isoelectronic defects is discussed by introducing a simple effective Hamiltonian. The results show a clear physical picture of what hole quenching means and yield qualitative conditions for when it will occur. The optical transition selection rules between a ground state and exciton states are also discussed for both cases. The electric-dipole interaction plays an important role for optical transitions of excitons bound to such isoelectronic defects, both for $J=\frac{3}{2}$ and $\frac{1}{2}$ holes. This is consistent with experimental facts, i.e., optical transitions from a ground state to a bound exciton (BE) singlet state in a singlet-triplet system (here the hole is quenched with total angular momentum $J=\frac{1}{2}$) and to BE $J=1$ states in a $J=\frac{3}{2}$ hole exciton system (a hole with $J=\frac{3}{2}$ and an electron with $S=\frac{1}{2}$ form $J=1$ and 2 BE states) are allowed. The effective-perturbation Hamiltonian model is also extended to discuss the first heavy–light-hole excitons in $GaAs/Al_{1-x}Ga_xAs$ quantum wells (QW's). The experimental data with magnetic fields up to 18 T from a 90-Å $GaAs/Al_{1-x}Ga_xAs$ QW have been analyzed, and g values of electrons and holes are obtained. To our knowledge, this is the first time that optical data of excitons in $GaAs/Al_{1-x}Ga_xAs$ QW's with magnetic fields have been analyzed in detail.

The paper is organized as follows: Section II gives a short description of the effective Hamiltonian. In Sec. III the isoelectronic defects and selection rules are discussed. Section IV gives a short discussion of excitons in quantum well. Section V is a summary.

II. EFFECTIVE-PERTURBATION HAMILTONIAN MODEL

The perturbation Hamiltonians for isoelectronic defects have been discussed in detail both for bulklike hole states[12] and spinlike hole states.[14] The perturbation Hamiltonians are constructed by assuming that the hole has angular momentum $J=\frac{3}{2}$ or $\frac{1}{2}$. The crystal-field potential is included in the perturbation Hamiltonian as an effective term. Instead, one can start from the original hole with orbital angular momentum $L=1$ and spin $S'=\frac{1}{2}$. The crystal field influences only the orbital momentum of holes. Therefore, for a defect with an axially symmetric potential, the effective Hamiltonian of the hole under a crystal-field perturbation can be written as[14]

$$H_1=-\tfrac{2}{3}\Delta\mathbf{L}\cdot\mathbf{S}-D'\left[L_z^2-\frac{L(L+1)}{3}\right]. \tag{1}$$

The first term describes spin-orbit interaction, and the parameter Δ is the spin-orbit splitting constant for a given host semiconductor. The second term describes the essential part of the axial potential. The parameter D' is given by the crystal potential strength. For a very strong crystal potential with low symmetry (where the symmetry is low enough to break all orbital angular momentum degeneracies of the hole), the qualitative discussion of hole quenching is given by Monemar, Lindefelt, and Chen.[15] For simplicity, only the effects of the defect potential along its main axis are considered in our discussion.

The eigenvalue equation for the effective-perturbation Hamiltonian (1) can be solved by using the following wave functions as a basis:

Γ_8 states,

$$\begin{aligned}
&|\tfrac{3}{2},-\tfrac{3}{2}\rangle=|1,-1\rangle\beta_h\ ,\\
&|\tfrac{3}{2},-\tfrac{1}{2}\rangle=(\tfrac{1}{3})^{1/2}|1,-1\rangle\alpha_h+(\tfrac{2}{3})^{1/2}|1,0\rangle\beta_h\ ,\\
&|\tfrac{3}{2},\tfrac{1}{2}\rangle=(\tfrac{2}{3})^{1/2}|1,0\rangle\alpha_h+(\tfrac{1}{3})^{1/2}|1,1\rangle\beta_h\ ,\\
&|\tfrac{3}{2},\tfrac{3}{2}\rangle=|1,1\rangle\alpha_h\ ;
\end{aligned} \tag{2a}$$

Γ_7 states,

$$\begin{aligned}
&|\tfrac{1}{2},-\tfrac{1}{2}\rangle=(\tfrac{2}{3})^{1/2}|1,-1\rangle\alpha_h-(\tfrac{1}{3})^{1/2}|1,0\rangle\beta_h\ ,\\
&|\tfrac{1}{2},\tfrac{1}{2}\rangle=(\tfrac{1}{3})^{1/2}|1,0\rangle\alpha_h-(\tfrac{2}{3})^{1/2}|1,1\rangle\beta_h\ ,
\end{aligned} \tag{2b}$$

where α_h and β_h are spin-up and -down wave functions, respectively. $|1,m_l\rangle$ are orbital angular momentum wave functions.

The matrix elements of H_1 with this basis are

	$\lvert\frac{3}{2},-\frac{3}{2}\rangle$	$\lvert\frac{3}{2},-\frac{1}{2}\rangle$	$\lvert\frac{3}{2},\frac{1}{2}\rangle$	$\lvert\frac{3}{2},\frac{3}{2}\rangle$	$\lvert\frac{1}{2},-\frac{1}{2}\rangle$	$\lvert\frac{1}{2},\frac{1}{2}\rangle$
$\lvert\frac{3}{2},-\frac{3}{2}\rangle$	$-\Delta/3-D'/3$	0	0	0	0	0
$\lvert\frac{3}{2},-\frac{1}{2}\rangle$	0	$-\Delta/3+D'/3$	0	0	$-(2/9)^{1/2}D'$	0
$\lvert\frac{3}{2},\frac{1}{2}\rangle$	0	0	$-\Delta/3+D'/3$	0	0	$(2/9)^{1/2}D'$
$\lvert\frac{3}{2},\frac{3}{2}\rangle$	0	0	0	$-\Delta/3-D'/3$	0	0
$\lvert\frac{1}{2},-\frac{1}{2}\rangle$	0	$-(2/9)^{1/2}D'$	0	0	$2\Delta/3$	0
$\lvert\frac{1}{2},\frac{1}{2}\rangle$	0	0	$(2/9)^{1/2}D'$	0	0	$2\Delta/3$

The eigenvalues of the perturbation Hamiltonian (1) are

$$\begin{aligned}
E_1&=-\Delta/3-D'/3\ ,\\
E_2&=\Delta/6+D'/6-\tfrac{1}{2}[8\Delta^2/9+(\Delta/3-D')^2]^{1/2}\ ,\\
E_3&=\Delta/6+D'/6+\tfrac{1}{2}[8\Delta^2/9+(\Delta/3-D')^2]^{1/2}\ .
\end{aligned} \tag{3}$$

The wave functions corresponding to the eigenvalues are

$$\begin{aligned}
&\Psi_1=|\tfrac{3}{2},\pm\tfrac{3}{2}\rangle\ ,\\
&\Psi_{i-}=A_1(E_i)|\tfrac{3}{2},-\tfrac{1}{2}\rangle+A_2(E_i)|\tfrac{1}{2},-\tfrac{1}{2}\rangle\ ,\\
&\Psi_{i+}=-A_1(E_i)|\tfrac{3}{2},\tfrac{1}{2}\rangle+A_2(E_i)|\tfrac{1}{2},\tfrac{1}{2}\rangle\ ,
\end{aligned} \tag{4}$$

where

$$\begin{aligned}
A_1(E_i)&=\frac{3D'(2\Delta/3-E_i)}{\{D'^2[2D'^2+9(2\Delta/3-E_i)^2]\}^{1/2}}\ ,\\
A_2(E_i)&=\left[\frac{2D'^2}{[2D'^2+9(2\Delta/3-E_i)^2]}\right]^{1/2}\ ,
\end{aligned} \tag{5}$$

$i=2,3$.

E_1 corresponds to doubly degenerate $|\frac{3}{2},\pm\frac{3}{2}\rangle$ states. The eigenstates belonging to E_2 and E_3 are linear combinations of $|\frac{3}{2},\pm\frac{1}{2}\rangle$ and $|\frac{1}{2},\pm\frac{1}{2}\rangle$ states. When D' is zero, the eigenstates for E_2 and E_3 are original $|\frac{3}{2},\pm\frac{1}{2}\rangle$ and $|\frac{1}{2},\pm\frac{1}{2}\rangle$ wave functions, and E_1 and E_2 are degenerate. But when D' is not zero, the states $|\frac{3}{2},\pm\frac{1}{2}\rangle$ and $|\frac{1}{2},\pm\frac{1}{2}\rangle$ interact through the crystal potential characterized by D'. The mixing of $|\frac{3}{2},\pm\frac{1}{2}\rangle$ and $|\frac{1}{2},\pm\frac{1}{2}\rangle$ states strongly depends on the relative ratio D'/Δ. It is increasing with increasing absolute value of the ratio D'/Δ.

The variation of energy levels with D'/Δ is given in Fig. 1(a). The corresponding expansion coefficients of the E_2 and E_3 levels are shown in Figs. 1(b) and 1(c). Figure 2 shows the mixing between E_2 and E_3 states versus the ratio D'/Δ. From this figure we can see that for $|D'/\Delta|<0.5$ the mixing is less than 5%. This means we can neglect the coupling of E_2 and E_3 levels. Particularly for $D'>0$ the lowest hole level is E_1, which is not coupling with the E_3 level. When such holes form bound excitons with an electron, if the electron-hole interaction is much weaker than the crystal potential, it is good enough to describe the hole by using E_1 level wave functions. This is the case for hole-attractive isoelectronic defects (see Table II). We conclude that when $|D'|/\Delta<0.5$, it is a good approximation to assign a total angular momentum $J=\frac{3}{2}$ to the bound hole. The spin-orbit interaction parameters for a few common semiconductors are shown in Table I. By using those values in Table I, we can easily estimate the limit of crystal potential strength where the approximation of a $J=\frac{3}{2}$ bound hole is still valid.

The extreme case is $|D'|\gg\Delta$. When $-D'\gg\Delta$, $A_1(E_2)\approx(\frac{2}{3})^{1/2}$, and $A_2(E_2)\approx(\frac{1}{3})^{1/2}$, the wave functions corresponding to the doubly degenerate E_2 level are $|1,0\rangle\alpha_h$ and $|1,0\rangle\beta_h$. For the E_3 level, $A_1(E_3)\approx(\frac{1}{3})^{1/2}$ and $A_2(E_3)\approx(\frac{2}{3})^{1/2}$, and so the corresponding doubly degenerate wave functions are

$|1,-1\rangle\alpha_h$ and $|1,1\rangle\beta_h$. The states with wave functions $|1,0\rangle\alpha_h$ and $|1,0\rangle\beta_h$ behave like $S=\frac{1}{2}$ spinors along the crystal potential axis. Thus we reach the conclusion that when D' is negative (corresponding to a compressed crystal potential) the lowest hole level is E_2, and it has spin-like wave functions when $-D' \gg \Delta$. In this case the hole is referred to as quenched by the crystal potential. It is easy to show that when D' is positive, the crystal field cannot quench the hole's orbital angular momentum for an axial symmetry crystal potential perturbation. This is consistent with available experimental data.

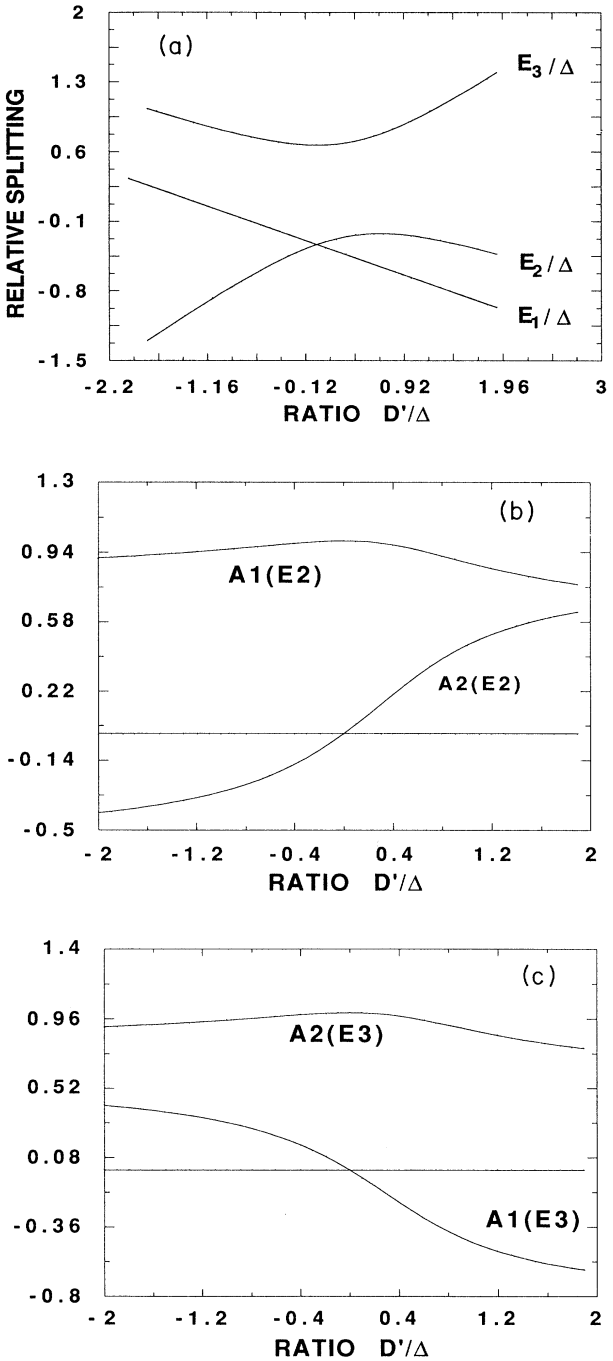

FIG. 1. (a) shows relative splitting between E_1, E_2, and E_3 with the ratio D'/Δ. Δ is the spin-orbit splitting constant of semiconductors. D' is a crystal-field parameter. (b) shows wave-function coefficients of $A_1(E_2)$ and $A_2(E_2)$ [see formula (4) in text] vs ratio D'/Δ. (c) shows wave-function coefficients of $A_1(E_3)$ and $A_2(E_3)$ [see formula (4) in text] vs ratio D'/Δ.

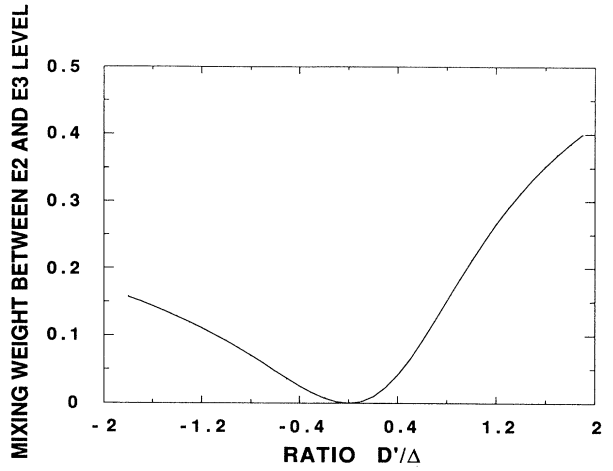

FIG. 2. Mixing of Γ_8 and Γ_7 wave functions for E_3 and E_2 level vs ratio D'/Δ.

III. ISOELECTRONIC DEFECTS

As shown in the previous section, when the crystal field is much weaker than the spin-orbit interaction, the hole can be treated as a particle with angular momentum $J=\frac{3}{2}$. Thus the crystal-field part in the Hamiltonian can be written as[4,14]

$$H_{\mathrm{LCF}}=D\left[J_z^2-\frac{J(J+1)}{3}\right]. \tag{6}$$

Here $J=\frac{3}{2}$, and the parameter D describes the effective strength of the crystal field. The perturbation Hamiltonian of isoelectronic defect bound excitons with $J=\frac{3}{2}$ holes has been discussed in detail before,[4] both with and without a magnetic field perturbation. Table II is a summary of the parameters a (the parameter a describes the electron-hole interaction) and D for various defects.

By comparing the splitting between E_1 and E_2 levels, one finds the relation $D'=6D(\Delta-2D)/(2\Delta-6D)$. The results in Table II show that the ratio $|D'|/\Delta$ satisfies the criterion $|D'|/\Delta<0.5$ for all centers listed there. This means that it is a good approximation to neglect interactions between Γ_8 and Γ_7 states.

Now we look at the selection rule for transitions of such defect bound excitons. Since the exciton state involves one electron and one hole, the zero-magnetic-field

TABLE I. Spin-orbit splitting of a few semiconductors.

	ZnTe	Si	GaP	GaAs
Spin-orbit splitting Δ (eV)	0.92	0.04	0.08	0.34
Reference	16	17	18	16

TABLE II. Parameters for a few isoelectronic defects.

	Electron attractive			Hole attractive			
	Li-Li-O bound exciton in GaP	NN_1 pair bound exciton in GaP	Be-related bound exciton in Si	Cu-related 2.329 eV in ZnTe	Cu-related 2.346 eV in ZnTe	Cu-related 2.26 eV in ZnTe *A*	*B*
Crystal fields D (meV)	1.66	0.20	0.48	120	−100	51.2	51.6
Electron and hole interaction a (meV)	0.77	0.585		0.02	0.06	0.22	0.20
Reference	5	4	10	8	9	6	

effective Hamiltonian can be written as[4,12,14]

$$H_{\mathrm{BE}}=-a\mathbf{J}\cdot\mathbf{S}-D\left[J_z^2-\frac{J(J+1)}{3}\right], \tag{7}$$

where $J=\frac{3}{2}$ is the angular momentum of a bound hole and $S=\frac{1}{2}$ for a spinlike bound electron. We form a basis with the following wave functions:

total angular momentum $J=1$ states,

$$\begin{aligned}
|1,1\rangle_J&=(\tfrac{3}{4})^{1/2}|\tfrac{3}{2},\tfrac{3}{2}\rangle\beta_e-(\tfrac{1}{4})^{1/2}|\tfrac{3}{2},\tfrac{1}{2}\rangle\alpha_e\ ,\\
|1,0\rangle_J&=(\tfrac{1}{2})^{1/2}|\tfrac{3}{2},\tfrac{1}{2}\rangle\beta_e-(\tfrac{1}{2})^{1/2}|\tfrac{3}{2},-\tfrac{1}{2}\rangle\alpha_e\ ,\\
|1,-1\rangle_J&=(\tfrac{1}{4})^{1/2}|\tfrac{3}{2},-\tfrac{1}{2}\rangle\beta_e-(\tfrac{3}{4})^{1/2}|\tfrac{3}{2},-\tfrac{3}{2}\rangle\alpha_e\ ;
\end{aligned} \tag{8}$$

total angular momentum $J=2$ states,

$$\begin{aligned}
|2,2\rangle_J&=|\tfrac{3}{2},\tfrac{3}{2}\rangle\alpha_e\ ,\\
|2,1\rangle_J&=(\tfrac{1}{4})^{1/2}|\tfrac{3}{2},\tfrac{3}{2}\rangle\beta_e+(\tfrac{3}{4})^{1/2}|\tfrac{3}{2},\tfrac{1}{2}\rangle\alpha_e\ ,\\
|2,0\rangle_J&=(\tfrac{1}{2})^{1/2}|\tfrac{3}{2},\tfrac{1}{2}\rangle\beta_e+(\tfrac{1}{2})^{1/2}|\tfrac{3}{2},-\tfrac{1}{2}\rangle\alpha_e\ ,\\
|2,-1\rangle_J&=(\tfrac{3}{4})^{1/2}|\tfrac{3}{2},-\tfrac{1}{2}\rangle\beta_e+(\tfrac{1}{4})^{1/2}|\tfrac{3}{2},-\tfrac{3}{2}\rangle\alpha_e\ ,\\
|2,-2\rangle_J&=|\tfrac{3}{2},-\tfrac{3}{2}\rangle\beta_e\ .
\end{aligned} \tag{9}$$

The eigenvalues of the Hamiltonian (7) are

$$\begin{aligned}
E(J=1;m=0)&=5a/4+D\ ,\\
E(\text{“}J=1\text{”};\text{“}m=\pm1\text{”})&=a/4+(D^2-aD+a^2)^{1/2}\ ,\\
E(J=2;m=0)&=-3a/4+D\ ,\\
E(\text{“}J=2\text{”};\text{“}m=\pm1\text{”})&=a/4-(D^2-aD+a^2)^{1/2}\ ,\\
E(J=2;m=\pm2)&=-3a/4-D\ .
\end{aligned} \tag{10}$$

The corresponding wave functions are

$$\begin{aligned}
&\Psi(J=1;m=0)=|1,0\rangle_J\ ,\\
&\Psi(J=2;m=0)=|2,0\rangle_J\ ,\\
&\Psi(J=2;m=\pm2)=|2,\pm2\rangle_J\ ,\\
&\Psi(\text{“}J=1\text{”};\text{“}m=\pm1\text{”})_+=-B_1(\text{“}J=1\text{”};\text{“}m=\pm1\text{”})|2,1\rangle_J+B_2(\text{“}J=1\text{”},\text{“}m=\pm1\text{”})|1,1\rangle_J\ ,\\
&\Psi(\text{“}J=1\text{”};\text{“}m=\pm1\text{”})_-=B_1(\text{“}J=1\text{”};\text{“}m=\pm1\text{”})|2,-1\rangle_J+B_2(\text{“}J=1\text{”};\text{“}m=\pm1\text{”})|1,-1\rangle_J\ ,
\end{aligned}$$

where

$$B_1(\text{“}J=1\text{”};\text{“}m=\pm1\text{”})=\frac{D[5a/2-D-2E(\text{“}J=1\text{”};\text{“}m=\pm1\text{”})]}{(D^2\{3D^2+[5a/2-D-2E(\text{“}J=1\text{”};\text{“}m=\pm1\text{”})]^2\})^{1/2}},$$

$$B_2(\text{“}J=1\text{”};\text{“}m=\pm1\text{”})=\left[\frac{3D^2}{\{3D^2+[5a/2-D-2E(\text{“}J=1\text{”};\text{“}m=\pm1\text{”})]^2\}}\right]^{1/2},$$

$$\Psi(\text{“}J=2\text{”};\text{“}m=\pm1\text{”})_+=-B_1(\text{“}J=2\text{”};\text{“}m=\pm1\text{”})|2,1\rangle_J+B_2(\text{“}J=2\text{”};\text{“}m=\pm1\text{”})|1,1\rangle_J,$$

$$\Psi(\text{“}J=2\text{”};\text{“}m=\pm1\text{”})_-=B_1(\text{“}J=2\text{”};\text{“}m=\pm1\text{”})|2,-1\rangle_J+B_2(\text{“}J=2\text{”};\text{“}m=\pm1\text{”})|1,-1\rangle_J, \tag{11}$$

where

$$B_1(\text{“}J=2\text{”};\text{“}m=\pm1\text{”})=\frac{D[5a/2-D-2E(\text{“}J=2\text{”};\text{“}m=\pm1\text{”})]}{(D^2\{3D^2+[5a/2-D-2E(\text{“}J=2\text{”};\text{“}m=\pm1\text{”})]^2\})^{1/2}},$$

$$B_2(\text{“}J=2\text{”};\text{“}m=\pm1\text{”})=\left[\frac{3D^2}{\{3D^2+[5a/2-D-2E(\text{“}J=2\text{”};\text{“}m=\pm1\text{”})]^2\}}\right]^{1/2}.$$

Once the eigenfunctions for the BE sublevels have been obtained, oscillator strengths for optical transitions between the BE substates and ground state (with no bound particles) can be calculated. Such oscillator strengths are proportional to the square of the electric-dipole matrix element:

$$M_{i0}=\langle\Psi_i|\mathbf{Q}|\Psi_0\rangle, \tag{12}$$

where $\mathbf{Q}$ is the dipole transition operator, Ψ_i is a particular BE substate, and Ψ_0 is the BE ground state.

With the notation S_s^m for total spin-wave functions (s is the total spin and m is the magnetic quantum number) of bound electrons and holes in the BE states, Eqs. (8) and (9) can be rewritten in terms of hole orbital angular momentum functions and total spin-wave functions:

$J=1$ states,

$$\begin{aligned}
|1,1\rangle_J&=(\tfrac{2}{3})^{1/2}|1,1\rangle S_0^0+(\tfrac{1}{6})^{1/2}[|1,1\rangle S_1^0-|1,0\rangle S_1^1],\\
|1,0\rangle_J&=(\tfrac{2}{3})^{1/2}|1,0\rangle S_0^0+(\tfrac{1}{6})^{1/2}[|1,1\rangle S_1^{-1}-|1,-1\rangle S_1^1],\\
|1,-1\rangle_J&=(\tfrac{2}{3})^{1/2}|1,-1\rangle S_0^0+(\tfrac{1}{6})^{1/2}[|1,0\rangle S_1^{-1}-|1,-1\rangle S_1^0];
\end{aligned} \tag{13}$$

$J=2$ states,

$$\begin{aligned}
|2,2\rangle_J&=|1,1\rangle S_1^1,\\
|2,1\rangle_J&=(\tfrac{1}{2})^{1/2}|1,1\rangle S_1^0+(\tfrac{1}{2})^{1/2}|1,0\rangle S_1^1,\\
|2,0\rangle_J&=(\tfrac{2}{3})^{1/2}|1,0\rangle S_1^0+(\tfrac{1}{6})^{1/2}[|1,1\rangle S_1^{-1}+|1,-1\rangle S_1^1],\\
|2,-1\rangle_J&=(\tfrac{1}{2})^{1/2}|1,-1\rangle S_1^0+(\tfrac{1}{2})^{1/2}|1,0\rangle S_1^{-1},\\
|2,-2\rangle_J&=|1,-1\rangle S_1^{-1}.
\end{aligned} \tag{14}$$

Since the electric-dipole operator influences only orbital angular momentum, the matrix elements are zero unless the total spin is the same in initial and final states and the difference in orbital angular momentum between initial and final states is ±1, i.e., $\Delta S=0$ and $\Delta L=\pm1$. In the BE ground state there are no particles, and so both the total orbital and spin angular momentums are zero; we denote this state as $|0,0\rangle$. This means that only $J=1$ states are electric-dipole-allowed final states in optical absorption experiments. One can calculate that

$$|\langle0,0|\mathbf{Q}|1,1\rangle_J|^2=|\langle0,0|\mathbf{Q}|1,0\rangle_J|^2=|\langle0,0|\mathbf{Q}|1,-1\rangle_J|^2=C\ (\text{const}) \tag{15a}$$

and

$$\begin{aligned}
|\langle0,0|\mathbf{Q}|2,2\rangle_J|^2&=|\langle0,0|\mathbf{Q}|2,1\rangle_J|^2=|\langle0,0|\mathbf{Q}|2,0\rangle_J|^2\\
&=|\langle0,0|\mathbf{Q}|2,-1\rangle_J|^2=|\langle0,0|\mathbf{Q}|2,-2\rangle_J|^2=0.
\end{aligned} \tag{15b}$$

To calculate relative oscillator strengths of optical transitions from the BE ground state ($|0,0\rangle$) to different substates of the BE, we let $C=1$, and we have

$$I(J=1;m=0)=|\langle 0,0|\mathbf{Q}|\Psi(J=1;m=0)\rangle|^2=C=1\ ,$$
$$I(\text{“}J=1\text{”};\text{“}m=\pm1\text{”})=|\langle 0,0|\mathbf{Q}|\Psi(\text{“}J=1\text{”};\text{“}m=\pm1\text{”})\rangle|^2=|B_2(\text{“}J=1\text{”};\text{“}m=\pm1\text{”})|^2C$$
$$=|B_2(\text{“}J=1\text{”};\text{“}m=\pm1\text{”})|^2\ ,$$

(16)

$$I(J=2;m=0)=|\langle 0,0|\mathbf{Q}|\Psi(J=2;m=0)\rangle|^2=0\ ,$$
$$I(\text{“}J=2\text{”};\text{“}m=\pm1\text{”})=|\langle 0,0|\mathbf{Q}|\Psi(\text{“}J=2\text{”};\text{“}m=\pm1\text{”})\rangle|^2=|B_2(\text{“}J=2\text{”};\text{“}m=\pm1\text{”})|^2C$$
$$=|B_2(\text{“}J=2\text{”};\text{“}m=\pm1\text{”})|^2\ ,$$
$$I(J=2;m=\pm2)=|\langle 0,0|\mathbf{Q}|\Psi(J=2;m=0)\rangle|^2=0\ .$$

The ratio of the oscillator between $E(\text{“}J=2\text{”};\text{“}m=\pm1\text{”})$ states and $E(\text{“}J=1\text{”};\text{“}m=\pm1\text{”})$ states is

$$R=I(\text{“}J=2\text{”},\text{“}m=\pm1\text{”})/I(\text{“}J=1\text{”},\text{“}m=\pm1\text{”})$$
$$=\frac{|B_2(\text{“}J=2\text{”};\text{“}m=\pm1\text{”})|^2}{|B_2(\text{“}J=1\text{”};\text{“}m=\pm1\text{”})|^2}=\frac{[2(D^2-aD+a^2)^{1/2}-(2a-D)]}{[2(D^2-aD+a^2)^{1/2}+(2a-D)]}\ . \tag{17}$$

We would like to point out that the formula (1) in Ref. 19 is the ratio of $|B_1(\text{“}J=1\text{”};\text{“}m=\pm1\text{”})|^2/|B_2(\text{“}J=1\text{”};\text{“}m=\pm1\text{”})|^2$; it should be given generally by formula (17) here. The relative oscillator strengths of different BE levels are shown in Fig. 3(b). The ratio R is shown in Fig. 4.

For defect centers which have even lower symmetry, formula (6) may give an insufficient description of crystal-field effects. It is necessary to introduce more terms,[4,12] but a discussion along the same line as here can be applied to these lower-symmetry cases.

When the crystal field is negative and satisfies $-D\gg\Delta$, the bound hole can be treated as a spinlike hole. If we consider only the isotropic electron-hole interaction, the perturbation Hamiltonian can be written as

$$H_{\mathrm{BE}}=-a(\mathbf{S}_h+\mathbf{L})\cdot\mathbf{S}_e\ . \tag{18a}$$

$\mathbf{L}$ and $\mathbf{S}_h$ are orbital angular momentum and spin operators for holes. $\mathbf{S}_e$ is the electron-spin operator. Corresponding wave functions are $|1,0\rangle\alpha_h$ and $|1,0\rangle\beta_h$ (this has been derived in Sec. II) for holes and α_e and β_e for electrons. We note that the $\mathbf{L}\cdot\mathbf{S}_e$ term can be neglected since it does not give any contribution to the total energy. This is the reason why a bound hole can be treated as a spinlike hole. So formula (18a) can be rewritten as

$$H_{\mathrm{BE}}=-a\mathbf{S}_h\cdot\mathbf{S}_e\ . \tag{18b}$$

Such spinlike electrons and holes interact to give singlet-triplet states.[14,20] The splitting between singlet and triplet states is $\Delta E=a$, and the corresponding wave functions of each state are as follows:
singlet state,

$$\Psi_0=(\tfrac{1}{2})^{1/2}|1,0\rangle(\alpha_h\beta_e-\beta_h\alpha_e)$$
$$=|1,0\rangle S_0^0\ ; \tag{19}$$

triplet states,

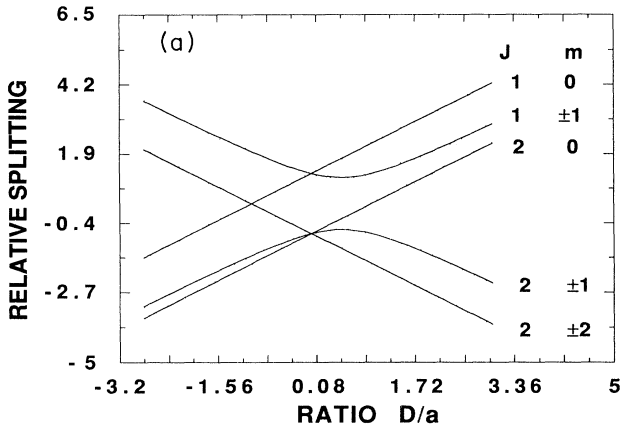

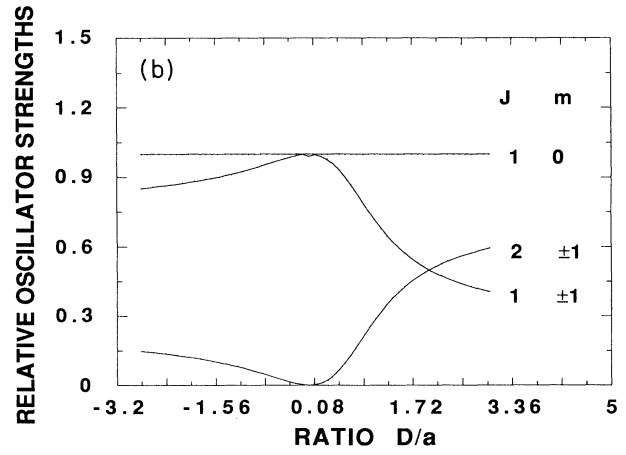

FIG. 3. (a) bound exciton energy-level splitting vs ratio D/a. (b) relative oscillator strengths of the electric-dipole-allowed transition bound exciton states vs ratio D/a.

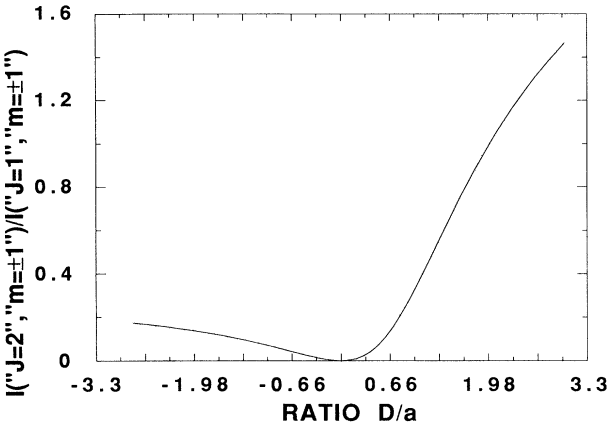

FIG. 4. Calculated ratio between the oscillator strengths of the substates "$m=\pm1$"("$J=2$") and "$m=\pm1$"("$J=1$") vs ratio D/a.

$$\Psi_{11}=|1,0\rangle\alpha_h\alpha_e=|1,0\rangle S_1^1 ,$$
$$\Psi_{10}=(\tfrac{1}{2})^{1/2}|1,0\rangle(\alpha_h\beta_e+\beta_h\alpha_e)$$
$$=|1,0\rangle S_1^0 , \tag{20}$$
$$\Psi_{1\text{-}1}=|1,0\rangle\beta_h\beta_e=|1,0\rangle S_1^{-1} .$$

According to the previous discussion on $J=\frac{3}{2}$ holes, the oscillator strengths of transitions from BE ground state to each of the BE states are as follows:
singlet state,

$$I_0=|\langle 0,0|\mathbf{Q}|\Psi_0\rangle|^2=\text{const} ; \tag{21}$$

triplet states,

$$I=|\langle 0,0|\mathbf{Q}|\Psi_{11}\rangle|^2$$
$$=\langle 0,0|\mathbf{Q}|\Psi_{10}\rangle|^2$$
$$=\langle 0,0|\mathbf{Q}|\Psi_{1\text{-}1}\rangle|^2=0 . \tag{22}$$

Here $|0,0\rangle$ is the BE ground state with no particles. $\mathbf{Q}$ is the electric-dipole operator. Electric-dipole transitions from the ground to the singlet state are allowed, and transitions to the triplet states are forbidden.

For moderately strong crystal fields, the mixing between Γ_8 and Γ_7 states must be taken into account, and it is not possible to assign a total angular momentum of $J=\frac{1}{2}$ or $\frac{3}{2}$ to the bound holes.

IV. QUANTUM-WELL STRUCTURES

Many sophisticated theories have been developed for calculating the electronic structures of quantum wells.[21] The following discussion for heavy–light-hole-related excitons gives a very clear physical understanding of the optical and magnetic properties of excitons in QW's. From a group-theoretical point of view, the problem of excitons in QW's is similar to an exciton bound to an isoelectronic defect with an axially symmetric potential. The discussion in Secs. II and III can be applied on heavy–light-hole excitons if we simulate the splitting between heavy and light holes by introducing an equivalent axial crystal-field potential, i.e., E_2-E_1 in formula (3). Figure 5 gives the dependence of the parameter D' on well width for single GaAs-$Al_{1-x}Ga_xAs$ QW's. If 5% mixing between Γ_8 and Γ_7 can be neglected, formulas (7)–(15) can be used to discuss the lowest heavy–light-hole exciton state in a single GaAs-$Al_{1-x}Ga_xAs$ QW. As derived from formulas (10), (11), and (15), we know that the heavy-hole exciton should split into two doubly degenerate states. Figure 6 shows a schematic picture of the electronic structure of excitons in a QW. The degeneracies of heavy-hole (HH) and light-hole (LH) excitons are lifted by electron-hole interaction (which is described by the parameter a), giving three doubly degenerate states (A, B, and D in Fig. 6) and two nondegenerate states (E and C in Fig. 6). The optical electric-dipole transitions from the exciton ground state (no particles in this state) to states B, D, and E are allowed and the transitions to A and C are forbidden. The relative oscillator strengths are given by formulas (15) and (16). The splitting between the heavy-hole exciton states A and B is in the order of 1 meV for 100-Å GaAs/$Al_{1-x}Ga_xAs$ QW's. This means that for high-quality QW samples at very low temperatures, double in photoluminescence spectra peaks of heavy-hole excitons can be observed since temperatures relax the electric-dipole transition rule. But, on the other hand, only one dominating absorption peak can be observed in absorption measurements because absorption follows the electric-dipole selection rule. This is consistent with the experimental data available.[22] The crystal-field strength parameter D can be determined by the splitting between light- and heavy-hole excitons, and the exchange splitting of the electron-hole pair can be determined by comparing the relative intensities of light- and heavy-hole exciton absorption. The degeneracies of BE states (A, B, and D) are lifted when an external magnetic field is applied. To understand the optical properties of heavy–light-hole-related excitons in a magnetic field, we introduce Zeeman terms in formula (7):

$$H=-a\mathbf{J}\cdot\mathbf{S}-D[J_z^2-J(J+1)/3]$$
$$+\mu_B(g_e\mathbf{B}\cdot\mathbf{S}+g_h\mathbf{B}\cdot\mathbf{J}) . \tag{23}$$

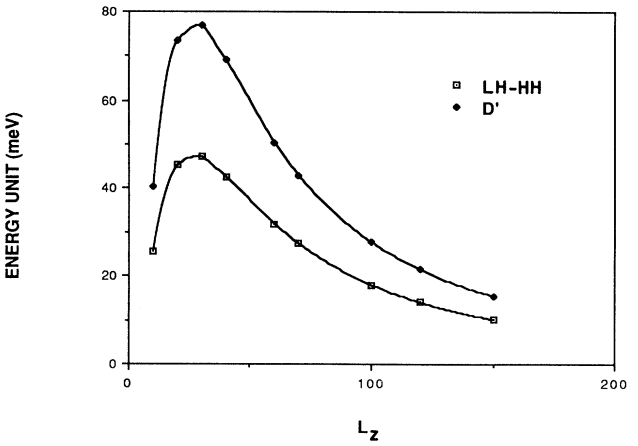

FIG. 5. Simulated D' parameter vs QW size L_z. The LH-HH curve gives the splitting between light- and heavy-hole states.

Here a is an electron-hole interaction parameter, D describes the splitting between the heavy- and light-hole excitons, g_e and g_h are g values of electrons and holes, μ_B is the Bohr magneton, and B is an applied magnetic field. If we apply a magnetic field along the QW growth direction, the B states of heavy-hole excitons and the D states of light-hole excitons mix. The corresponding eigenvalues of the Hamiltonian (23) are as follows:
heavy-hole exciton states,

$$E_A(B)=-3a/4-D+\mu_B B(g_e/2+3g_h/2)\ ,$$
$$E_A(B)=-3a/4-D-\mu_B B(g_e/2+3g_h/2)\ ; \tag{24}$$

light-hole states,

$$E_E(B)=5a/4+D\ ,$$
$$E_C(B)=-3a/4+D\ ; \tag{25}$$

mixed states between heavy- and light-hole excitons,

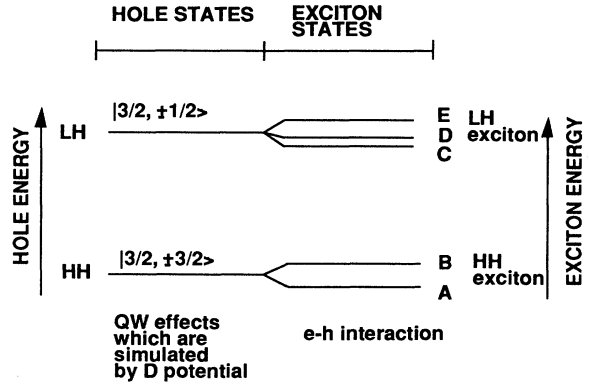

FIG. 6. Schematic picture of the electronic structure for the heavy–light-hole-related excitons in a $GaAs/Al_{1-x}Ga_xAs$ QW.

$$E_{1,2}(B)=\frac{[A+E_D(B=0)+A'+E_B(B=0)]}{2}\pm\frac{\{[A+E_D(B=0)-A'-E_B(B=0)]^2+4F^2\}^{1/2}}{2}\ ,$$
$$E_{3,4}(B)=\frac{[-A+E_D(B=0)-A'+E_B(B=0)]}{2}\pm\frac{\{[A-E_D(B=0)-A'+E_B(B=0)]^2+4F^2\}^{1/2}}{2}\ . \tag{26}$$

The new parameter in these eigenvalues are

$$E_D(B=0)=\frac{a}{4}+(D^2-aD+a^2)^{1/2}\ ,$$
$$E_B(B=0)=\frac{a}{4}-(D^2-aD+a^2)^{1/2}\ ,$$
$$A=\frac{B_1(J=1;m=\pm1)^2(-g_e-3g_h)\mu_B B}{4}+\frac{B_2(J=1;m=\pm1)^2(g_e-5g_h)\mu_B B}{4}\ ,$$
$$A'=\frac{B_1(J=2;m=\pm1)^2(-g_e-3g_h)\mu_B B}{4}+\frac{B_2(J=2;m=\pm1)^2(g_e-5g_h)\mu_B B}{4}\ ,$$
$$F=\frac{B_1(J=1;m=\pm1)B_1(J=2;m=\pm1)(-g_e-3g_h)\mu_B B}{4}+\frac{B_2(J=2;m=\pm1)B_2(J=1;m=\pm1)(g_e-5g_h)\mu_B B}{4}\ ,$$
$$B_1(J=1;m=\pm1)=\frac{[5a/2-D-2E_D(B=0)]D}{(D^2\{3D^2+[5a/2-D-2E_B(B=0)]^2\})^{1/2}}\ ,$$
$$B_2(J=1;m=\pm1)=\left[\frac{3D^2}{\{3D^2+[5a/2-D-2E_D(B=0)]^2\}}\right]^{1/2}\ ,$$
$$B_1(J=2;m=\pm1)=\frac{[5a/2-D-2E_B(B=0)]D}{(D^2\{3D^2+[5a/2-D-2E_B(B=0)]^2\})^{1/2}}\ ,$$
$$B_2(J=2;m=\pm1)=\left[\frac{3D^2}{\{3D^2+[5a/2-D-2E_B(B=0)]^2\}}\right]^{1/2}\ .$$

In Fig. 7 the Zeeman splitting pattern of heavy–light-hole excitons with magnetic fields up to 18 T is shown. The data points are experimental results from Ref. 22, where center shifting of each state with magnetic field is removed. A least-squares fitting procedure between

TABLE III. Parameters of C_1 and C_2.

	C_1 (meV/T)	C_2 (meV/T^2)
A	0.1499	0.0178
B	0.2102	0.0160

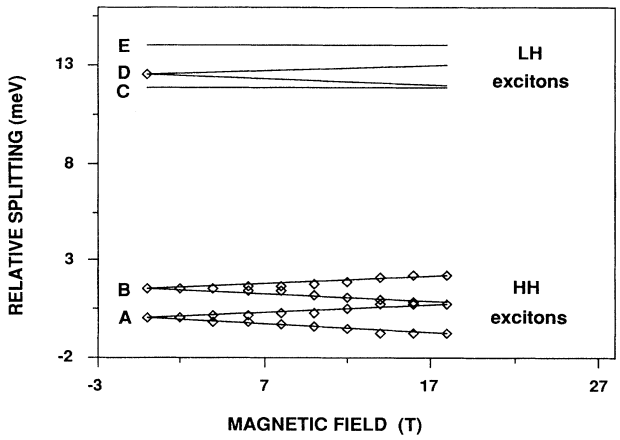

FIG. 7. Fan diagram of excitons for a 90-Å $GaAs/Al_{0.26}Ga_{0.74}As$ QW with magnetic field from 0 to 18 T in the layer growth direction. The solid lines are computed from formulas (24)–(26) in the text. Squares correspond to the experimental results after removing center shift with magnetic field (experimental data from Ref. 22).

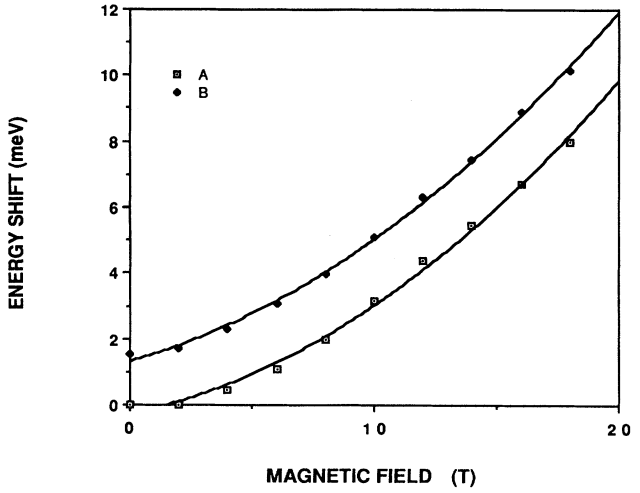

FIG. 8. The center magnetic shift of A and B states in Fig. 6. Solid lines are computed from formula (22) in text, and squares are experimental data (Ref. 22).

theory and experimental results gives the following parameters for a 90-Å $GaAs/Al_{0.26}Ga_{0.74}As$ QW:

$$a = 1.05 \pm 0.02 \text{ meV} ,$$

$$D = 5.95 \pm 0.02 \text{ meV} ,$$

$$g_e = -0.26 \pm 0.05 ,$$

$$g_h = 0.58 \pm 0.05 .$$

The center shifting of the two components (A and B) of heavy-hole excitons with magnetic field is shown in Fig. 8. The points are experimental results from Ref. 22, and the solid curves are calculated from formula (27) and parameters in Table III:

$$\Delta E(B) = C_1 B + C_2 B^2 . \quad (27)$$

The coefficient C_1, which describes a linear shifting with magnetic field B, is zero for excitons in bulk materials. A nonzero c_1 is characteristic of two-dimensional (2D) carriers. The origin of C_1 is Landau splitting of 2D carrier energy levels in a perpendicular magnetic field. The diamagnetic shift parameter C_2 is close to the value for bulk GaAs (0.02 meV/T^2).

V. SUMMARY

In summary, the properties of isoelectronic defect bound excitons in semiconductors have been discussed. The quenching mechanisms of bound holes are due to the strong negative crystal-field perturbation for an axially symmetric potential, since the crystal-field perturbation causes mixing between Γ_8 and Γ_7 symmetry wave functions for holes. The selection rule for BE recombination with electric-dipole interaction has also been examined; the results show that electric-dipole transitions to $J=1$ states for $J=\frac{3}{2}$ holes and transitions to a $S=0$ state for spinlike hole isoelectronic defect bound excitons are allowed. By extending this simple model to quantum-well structures, the optical and electronic properties of the first heavy- and light-hole excitons can be easily understood. The g values of electrons and holes in quantum wells are obtained by fitting experimental results.

ACKNOWLEDGMENTS

One of us (Q.X.Z.) wishes to thank NTNF in Norway for financial support and gratefully acknowledges fruitful discussions with Professor Bo Monemar on isoelectronic defect problems during his (Q.X.Z.) stay in Linkoping University in Sweden.

[1]D. G. Thomas and J. J. Hopfield, Phys. Rev. **150**, 680 (1966).
[2]E. Cohen, M. D. Sturge, W. O. Lipari, M. Altarelli, and A. Baldereschi, Phys. Rev. Lett. **35**, 1591 (1975).
[3]J. D. Cuthbert, C. H. Henry, and P. J. Dean, Phys. Rev. **170**, 739 (1968).
[4]Q. X. Zhao and B. Monemar, Phys. Rev. B **38**, 1397 (1988).
[5]Q. X. Zhao, P. Bergman, and B. Monemar, Phys. Rev. B **3** 8383 (1988).
[6]B. Monemar, P. O. Holtz, W. M. Chen, H. P. Gislason, U. Lindefelt, and M. E. Pistol, Phys. Rev. B **34**, 8656 (1986).
[7]B. Monemar, P. O. Holtz, H. P. Gislason, N. Magnea, Ch. Uihlein, and P. L. Liu, Phys. Rev. B **32**, 3844 (1985).
[8]Q. X. Zhao, B. Monemar, and P. O. Holtz, Phys. Rev. B **36**, 3331 (1987).

[9]W. M. Chen, Q. X. Zhao, B. Monemar, H. P. Gislason, and P. O. Holtz, Phys. Rev. B **33**, 3722 (1987).
[10]N. Killoran, D. J. Dunstan, M. O. Henry, E. C. Lightowlers, and B. C. Cavenett, J. Phys. C **15**, 6067 (1982).
[11]P. O. Holtz, Q. X. Zhao, and B. Monemar, Phys. Rev. B **36**, 5051 (1987).
[12]Q. X. Zhao, Ph.D. thesis, Linkoping University, 1988.
[13]J. J. Hopfield, R. G. Thomas, and R. T. Lynch, Phys. Rev. Lett. **17**, 312 (1966).
[14]A. Abragam and B. Bleaney, *Electron Paramagnetic Resonance of Transition Metal Ions* (Clarendon, Oxford, 1970).
[15]B. Monemar, U. Lindefelt, and W. M. Chen, Physica B+C **146B**, 256 (1987).
[16]M. Cardona, K. L. Shaklee, and F. H. Pollack, Phys. Rev. **154**, 696 (1967).
[17]C. S. Zwerdling, K. J. Button, B. Lax, and L. M. Roth, Phys. Rev. Lett. **4**, 173 (1960).
[18]P. J. Dean, G. Kaminsky, and R. B. Zettersirom, J. Appl. Phys. **38**, 3551 (1969).
[19]P. J. Dean, Phys. Rev. B **4**, 2596 (1971).
[20]W. M. Chen, Ph.D. thesis, Linkoping University, 1987.
[21]G. Bastard, *Wave Mechanics Applied to Semiconductor Heterostructures* (Les Editions de Physique, Paris, 1987).
[22]M. Potemski, J. C. Maan, A. Fasolino, K. Ploog, and G. Weimann (unpublished).